Polymer 51 (2010) 1124–1132

Contents lists available at ScienceDirect

Polymer

journal homepage: www.elsevier.com/locate/polymer

# Morphology and thermomechanical properties of main-chain polybenzoxazine-*block*-polydimethylsiloxane multiblock copolymers

Lei Wang, Sixun Zheng*

*Department of Polymer Science and Engineering and State Key Laboratory of Metal Matrix Composites, Shanghai Jiao Tong University, Shanghai 200240, PR China*

ARTICLE INFO

*Article history:*
Received 25 August 2009
Received in revised form
29 December 2009
Accepted 6 January 2010
Available online 18 January 2010

*Keywords:*
Polybenzoxazine
Polydimethylsiloxane
Multiblock copolymer

ABSTRACT

The main-chain polybenzoxazine-*block*-polydimethylsiloxane multiblock copolymers were synthesized *via* the Mannich polycondensation among 4,4′-dihydroxyldiphenylisopropane, 4,4′-diaminodiphenylmethane, aminopropyl-terminated polydimethylsiloxane and paraformaldehyde. The multiblock copolymers were characterized by means of Fourier transform infrared spectroscopy (FTIR), nuclear magnetic resonance spectroscopy (NMR) and size exclusion chromatography (SEC). Atomic force microscopy (AFM) and small-angle X-ray scattering (SAXS) showed that the multiblock copolymers displayed microphase-separated morphology. Owing to the presence of the main-chain polybenzoxazine blocks, the multiblock copolymers are thermally-crosslinkable. The curing behavior of the multiblock copolymers was investigated according to the analysis of non-isothermal curing kinetics. The measurement of static contact angles showed that with the inclusion of polydimethylsiloxane blocks, the polybenzoxazine thermosets resulting from the multiblock copolymers displayed the improved surface hydrophobicity.



## 1. Introduction

Polybenzoxazines (PBa) are a class of attractive alternatives to some traditional thermosets such as epoxies, phenolic resins, bismaleimides owing to their excellent thermal, mechanical properties and electrical properties [1]. The thermosetting polymers can be prepared *via* thermally-activated ring-opening polymerization of benzoxazine monomers and no hardeners are required involving the curing process [2–4]. The unique chemistry of polymerization endows the materials with excellent processing properties through a very wide range of molecular design. Generally, the monomers of PBa can be readily prepared *via* Mannich condensation among phenols, formaldehyde and primary amines either in solution or in melt state [5]. Depending on the functionalities of phenolic compounds and primary amines, mono-, bi- and even multifunctional precursors of benzoxazine can be obtained. During the past decade, a variety of low-molecular-weight precursors have been synthesized by the use of a monofunctional phenol (and/or a bifunctional phenol) and a bifunctional amine (and/or a monoamine) [6–23]. It has been noted that the curing process of low-molecular-weight precursors would be accompanied with the thermal dissociation of the monomers, which was always competing with the chain propagation [4,19]. The utilization of polyfunctional benzoxazine precursors could provide the thermosets with high structural integrity and thus the materials would possess improved properties (*e.g.*, mechanical and physical properties) and processability (*e.g.*, film-forming properties) [24–26]. Takeichi et al. [24] have reported the synthesis of high-molecular-weight precursors by using the Mannich polycondensation among a bifunctional phenol (*e.g.*, bisphenol A), a diamine (*e.g.*, ethylenediamine or hexamethylenediamine) and formaldehyde. Alternatively, the high-molecular-weight precursors with oxazine ring in the main chains were prepared *via* the polycondensation between aminophenols and formaldehyde [25]. It was found that the transparent thin films of the high-molecular-weight precursors were easily obtained by solution casting approach using the solution of precursors and the cured polybenzoxazine films exhibited significantly improved toughness than those from the curing of benzoxazine monomers [24–26].

The potential applications of PBa thermosets motivate to prepare the materials with improved properties. Multiblock copolymers can display a wide spectrum of morphological structures and properties depending on the type and volume fraction of their component blocks. An important approach to modify the materials is to prepare block copolymers with combined properties. In this work, we reported the synthesis of a multiblock copolymer consisting of main-chain polybenzoxazine and polydimethylsiloxane blocks *via* Mannich polycondensation. Owing to the presence of the main-chain polybenzoxazine subchains, the multiblock copolymer can be

* Corresponding author. Tel.: +86 21 54743278; fax: +86 21 54741297.
*E-mail address:* szheng@sjtu.edu.cn (S. Zheng).

0032-3861/$ – see front matter © 2010 Elsevier Ltd. All rights reserved.
doi:10.1016/j.polymer.2010.01.008

crosslinked *via* thermally activated polymerization. In the multiblock copolymer, the chemically-incorporated PDMS was microphase-separated out and acted as the nanophases to improve thermomechanical properties of the PBa thermosets. The approach is quite different from the traditional approaches to modify the thermosets *via* physical blending. In fact, simple physical blending with organosilicon polymer (*e.g.*, PDMS) is not successful for the modification of the PBa thermosets owing to the poor miscibility of PBa with polysiloxanes and thus a variety of chemical techniques would be employed to avoid macroscopic phase separation [27–32]. Takeichi et al. [27] have ever reported the synthesis of tough high molecular weight benzoxazines precursors containing siloxane. They also reported the modification of PBa thermosets with organosilicon polymers *via* sol-gel process [28,29] and physical blending with poly(imide-*co*-siloxane) copolymer [30]. More recently, Yagci et al. [31] synthesized the oligosiloxanes containing benzoxazine moieties in the main chain by hydrosilylation reaction between tetramethyldisiloxane and benzoxazines structurally equipped with allyl groups.

In this work, we firstly presented synthesis of the PBaDDM-*block*-PDMS multiblock copolymers *via* the Mannich polycondensation among 4,4′-dihydroxyldiphenylisopropane, 4,4′-diaminodiphenylmethane, aminopropyl-terminated polydimethylsiloxane and paraformaldehyde. Thereafter, the morphology and thermal properties of the multiblock copolymers will be investigated by means of atomic force microscopy (AFM), small-angle X-ray scattering (SAXS) and thermal gravimetric analysis (TGA). The curing behavior of the multiblock copolymer was addressed on the basis of non-isothermal curing kinetics by means of differential scanning calorimetry (DSC).

## 2. Experimental

### 2.1. Materials

4,4′-Dihydroxyldiphenylisopropane (BPA) and 4,4′-diaminodiphenylmethane (DDM) were of analytical pure grade, purchased from Shanghai Reagent Co., China. Paraformaldehyde was obtained from Aldrich Co., USA. Aminopropyl-terminated polydimethylsiloxane ($NH_2$–PDMS–$NH_2$) was kindly supplied by Degussa Co. Germany and it has a quoted number-average molecular weight of $M_n = 2300$. Prior to use, it was dried *via* azeotropic distillation with anhydrous toluene. The solvents such as chloroform and toluene were obtained from commercial source; they were purified with standard procedures prior to use. The plain PBaDDM was synthesized by following the method reported by Takeichi et al. [24] and it has the intrinsic viscosity of $[\eta] = 0.33$ dL/g measured in chloroform solution at 30 °C with a Ubbelohde viscometer.

### 2.2. Synthesis of PBaDDM-b-PDMS multiblock copolymers

Typically, BPA (4.202 g, 18.43 mmol), DDM (3.121 g, 15.74 mmol) and a suspension of paraformaldehyde (2.262 g) dispersed in 40 mL chloroform were charged to a flask equipped with a reflux condenser and a magnetic stirrer. The reactive mixture was refluxed for 5 h with vigorous stirring and then the $NH_2$–PDMS–$NH_2$ (5.714 g, 2.69 mmol) and paraformaldehyde (0.388 g) were added. The Mannich polycondensation was carried out at 85 °C for 12 h. Cooled to room temperature, the insoluble component (*i.e.*, unreacted paraformaldehyde) was removed with filtration and the solution was dropped into an excessive amount of cold methanol to afford the yellow precipitates. The crude polymers were re-dissolved in chloroform and then precipitated in an excessive amount of cold methanol. This procedure was repeated three times to purify the samples. The samples were further dried at 40 °C in a vacuum oven for 24 h and the resulting product (12.13 g) was obtained with the yield of 87%. The molecular weight of the block copolymer was also measured by means of gel permeation chromatography (GPC) to be $M_n = 6840$ with $M_w/M_n = 2.34$. FTIR (KBr window, $cm^{-1}$): 1234 (C–O–C of oxazine), 1188 (C–N–C of oxazine). $^1$H NMR ($CDCl_3$, ppm): 0.08 (*t*, 6.18H, Si–C**H**$_3$), 1.57 (*d*, 3.02H, –C**H**$_3$), 3.79 (*s*, 1.00H, Ar–C**H**$_2$–Ar), 4.52 [*s*, 1.40H, Ar–C**H**$_2$–N (oxazine ring)], 5.28 [*s*, 1.42H, O–C**H**$_2$–N (oxazine ring)], 6.8–7.2 (*m*, 6.44H, protons of aromatic ring).

### 2.3. Measurement and techniques

#### 2.3.1. Nuclear magnetic resonance spectroscopy (NMR)

The $^1$H NMR measurement was carried out on a Varian Mercury Plus 400 MHz NMR spectrometer at 25 °C. The samples were dissolved with deuterated chloroform ($CDCl_3$) and the solutions were measured with tetramethylsilane (TMS) as an internal reference.

#### 2.3.2. Fourier transform infrared spectroscopy (FTIR)

The FTIR measurements were conducted on a Perkin–Elmer Paragon 1000 Fourier transform spectrometer at room temperature (25 °C). The specimens of the films were obtained *via* casting the chloroform solution of the samples (2 wt%) onto KBr windows. The majority of solvent was evaporated at room temperature for 1 h and the residual solvent was eliminated by drying the specimens *in vacuo* at 30 °C for 48 h before use. All the films were sufficiently thin to be within a range where the Beer–Lambert law is obeyed. In all cases, 32 scans at a resolution of 4 $cm^{-1}$ were used to record the spectra.

#### 2.3.3. Size exclusion chromatography (SEC)

The molecular weights of polymers were determined on a Waters 717 Plus autosampler gel permeation chromatography apparatus equipped with Waters RH columns and a Dawn Eos (Wyatt Technology) multi-angle laser light scattering detector and the measurements were carried out at 25 °C with tetrahydrofuran as the eluent at the rate of 1.0 mL/min.

#### 2.3.4. Small-angle X-ray scattering (SAXS)

The SAXS measurements were taken on a Bruker Nanostar system. Two dimensional diffraction patterns were recorded using an image intensified CCD detector. The experiments were carried out at room temperature (25 °C) using Cu-Ka radiation ($\lambda = 1.54$ Å, wavelength) operating at 40 kV, 35 mA. The profiles of intensity were output as the plot of scattering intensity ($I$) versus scattering vector, $q = (4/\lambda)\sin(\theta/2)$ ($\theta$ = scattering angle).

#### 2.3.5. Atomic force microscopy (AFM)

The thermosets were trimmed using an ultrathin microtome machine, and the sections of specimens (*ca.* 70 nm in thickness) were used for AFM observations. The AFM experiments were performed with a Nanoscope IIIa scanning probe microscope (Digital Instruments, Santa Barbara, CA). Tapping mode was employed in air using a tip fabricated from silicon (125 μm in length with *ca.* 500 kHz resonant frequency). Typical scan speeds during recording were 0.3–1 lines $s^{-1}$ using scan heads with a maximum range of 1 μm × 1 μm.

#### 2.3.6. Differential scanning calorimetry (DSC)

Thermal analysis was performed on a TA Instruments Q2000 differential scanning calorimeter in a dry nitrogen atmosphere. The instrument was calibrated with a standard indium. To investigate the non-isothermal curing kinetics, the specimens were heated from 140 to 300 °C at five different heating rates of 2, 5, 10, 15 and 20 °C/min, respectively.

*2.3.7. Thermo gravimetric analysis (TGA)*

A TA Instruments Q5000 thermalgravimetric analyzer was used to investigate the thermal stability of the multiblock copolymers. All of the thermal analyses were conducted in nitrogen atmosphere from ambient temperature to 800 °C at the heating rate of 20 °C/min. The thermal degradation temperature was taken as the onset temperature at which 5 wt% of weight loss occurs.

*2.3.8. Surface contact angle analysis*

The specimens for surface contact angle analysis were prepared *via* spin-coating of the THF solutions of the polymers onto glass slider and the thickness of the films was controlled to be at least 25 μm to avoid the possible effect of the glass matrix on the measurements. The flat free surfaces of the thermosets were used for the measurement of contact angle. The static contact angle measurements with the probe liquids (*i.e.*, ultrapure water and ethylene glycol) were carried out on a KH-01-2 contact angle measurement instrument (Beijing Kangsente Scientific Instruments Co., China) at room temperature. The samples were dried at 60 °C in a vacuum oven for 24 h prior to measurement.

## 3. Result and discussion

*3.1. Synthesis of PBaDDM-b-PDMS multiblock copolymers*

The synthetic route for PBaDDM-*b*-PDMS multiblock copolymers is shown in Scheme 1. In the first step, the Mannich polycondensation among 4,4′-dihydroxyldiphenylisopropane (BPA), 4,4′-diaminodiphenylmethane (DDM) and paraformaldehyde was carried out in their solution of chloroform by following the approach reported by Takeichi et al. [24]. The polycondensation afforded the phenolic hydroxyl-terminated polybenzoxazine prepolymer (*viz.* HO–PBaDDM–OH) while 4,4′-dihydroxyldiphenylisopropane was excess. Thereafter, the aminopropyl-terminated polydimethylsiloxane ($NH_2$–PDMS–$NH_2$) was added to the system to continue the Mannich condensation and to obtain PBaDDM-*b*-PDMS multiblock copolymers. It should be pointed out that in the above two-step polycondensation, the molar ratios of phenolic hydroxyl groups (from BPA) to amino groups (from DDM and aminopropyl-terminated PDMS) were controlled to be 1:1. By adjusting the quantity of aminopropyl-terminated polydimethylsiloxane, the multiblock copolymers containing variable amount of PDMS were obtained. It was observed that with the polymerization proceeding, the viscosity of the reactive system increased significantly; the polymerization was carried out for 12 h to perform the reaction to completion. The feed ratios and the molecular weights of the multiblock copolymers were summarized in Table 1. Representatively shown in Fig. 1 is the Fourier transform infrared spectrum (FTIR) of PBaDDM54-*b*-PDMS. The bands at 1188 and 1234 $cm^{-1}$ are assignable to the asymmetric stretching vibration of C–N–C and C–O–C moieties of oxazine ring and the band at 1326 $cm^{-1}$ is ascribed to the wagging vibration of methylene groups of oxazine ring. The stretching vibration of Si–O–Si bond is detected at 1097 $cm^{-1}$ and the symmetric deformation vibration of Si–$CH_3$ bonds was observed at 1261 $cm^{-1}$ in addition to the characteristic bands of PBaDDM blocks at 1188, 1234 and 1326 $cm^{-1}$. The FTIR spectroscopy indicates that the resulting product combined the structural features from PBaDDM and PDMS blocks. The $^1H$ NMR spectrum of PBaDDM54-*b*-PDMS was presented in Fig. 2. The signals of resonance at 4.52 and 5.28 ppm are assignable to the proton of methylene groups of benzoxazine rings. The resonance at 1.58 ppm is ascribed to the protons of methyl groups in the moiety of bisphenol A whereas the signal of resonance at 3.79 ppm to the

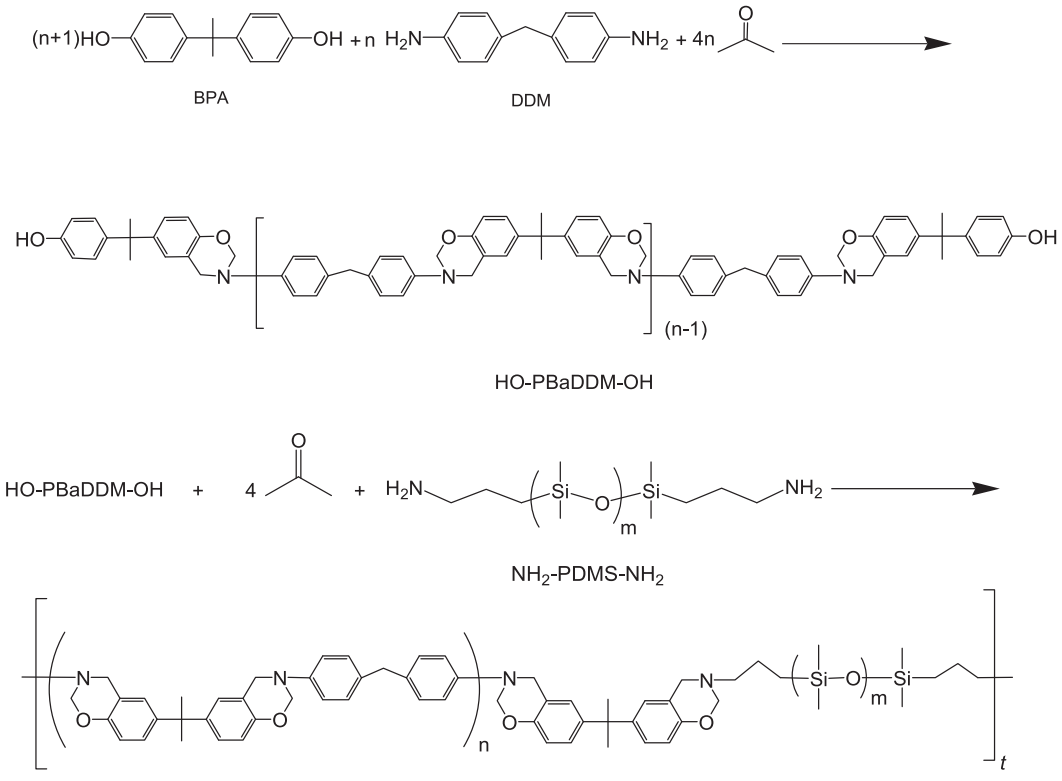


PBaDDM-*block*-PDMS Multiblock Copolymer

**Scheme 1.** Synthesis of PBaDDM-*b*-PDMS multiblock copolymer.

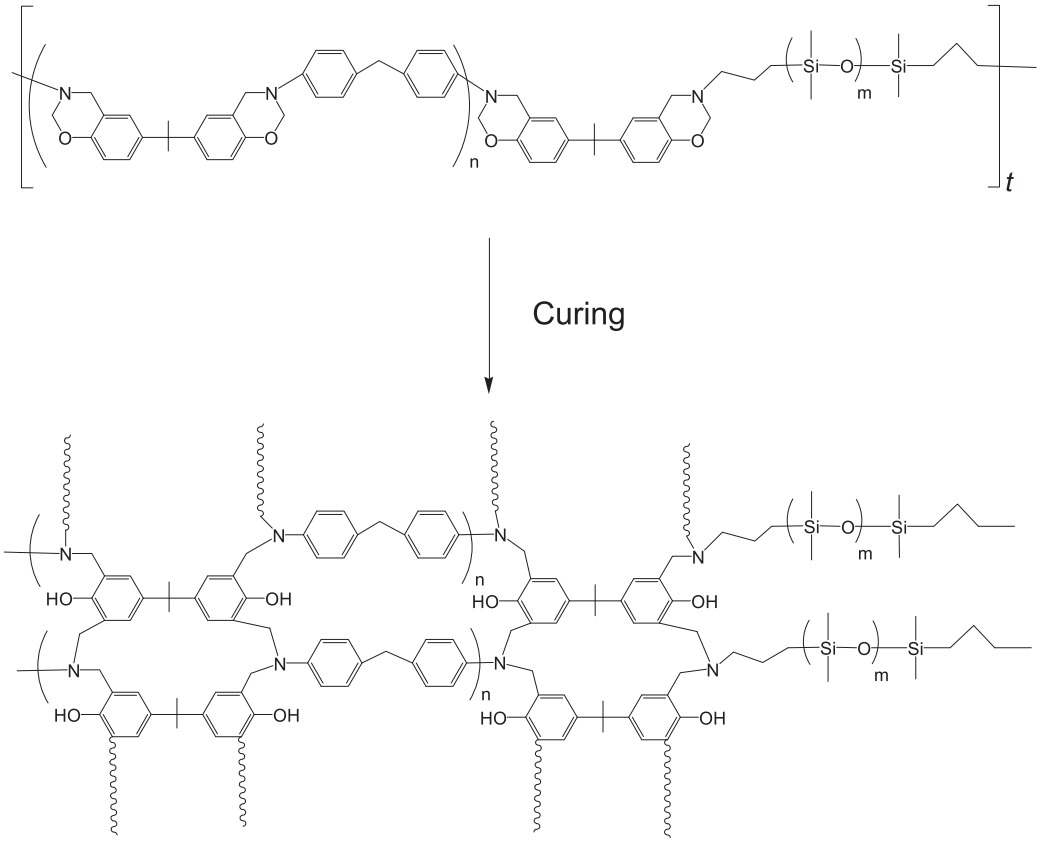


**Scheme 2.** Thermal curing of PBaDDM-*b*-PDMS multiblock copolymers.

protons of methylene groups in 4,4′-diaminodiphenylmethane moiety. The resonance in the range of 6.9–7.2 ppm was attributed to the protons of aromatic rings in the backbone of PBaDDM macromers. According to the ratio of integration intensity of the resonance at 1.5 ppm to that at 3.79 ppm, it was judged that the molar ratio of BPA to DDM moiety in the macromer followed that feed ratio of BPA to DDM, implying that the Mannich condensation has been performed to completion under the present condition of reaction. The PDMS block is characteristic of the resonance signals of protons at 0.08, 1.01 and 2.28 ppm, which are assignable to the protons of the methyl groups, the methylene connected to silicon atom and the methylene connected to amino groups of PDMS blocks. This result indicates the resulting polymer possessed the structural features from both PBaDDM and PDMS blocks. The gel permeation chromatography (GPC) was used to measure the molecular weights of PBaDDM-*b*-PDMS multiblock copolymers and the GPC curves were showed in Fig. 3. All the GPC curves displayed unimodal peaks, suggesting that the polymerization has been performed to completion. In another word, there are no detectable unreacted macromers (*i.e.,* HO–PBaDDM–OH and $NH_2$–PDMS–$NH_2$). The multiblock copolymers with the molecular weights of 4560–7730 were obtained and the polydispersity of the multiblock copolymers is fairly broad, ranging from 2.31 to 2.86. This result could be associated with the decreased

**Table 1**
Feed ratios and molecular weights of PBaDDM-*b*-PDMS multiblock copolymers.

| Samples[a] | [BPA]:[DDM]:[PDMS][b] | PDMS (wt%) | $M_n$[c] | $M_w/M_n$[c] |
|---|---|---|---|---|
| PBaDDM28-*b*-PDMS | 7.88:4.88:3.00 | 71.7 | 4560 | 2.31 |
| PBaDDM45-*b*-PDMS | 11.84:9.34:2.50 | 55.8 | 7800 | 2.52 |
| PBaDDM54-*b*-PDMS | 18.43:15.74:2.69 | 45.8 | 6840 | 2.34 |
| PBaDDM61-*b*-PDMS | 13.43:11.93:1.50 | 38.9 | 7730 | 2.86 |

[a] Digits following "PBaDDM" represent the weight fraction of PBaDDM in the copolymers.
[b] Molar ratio of reactants.
[c] Determined with GPC.

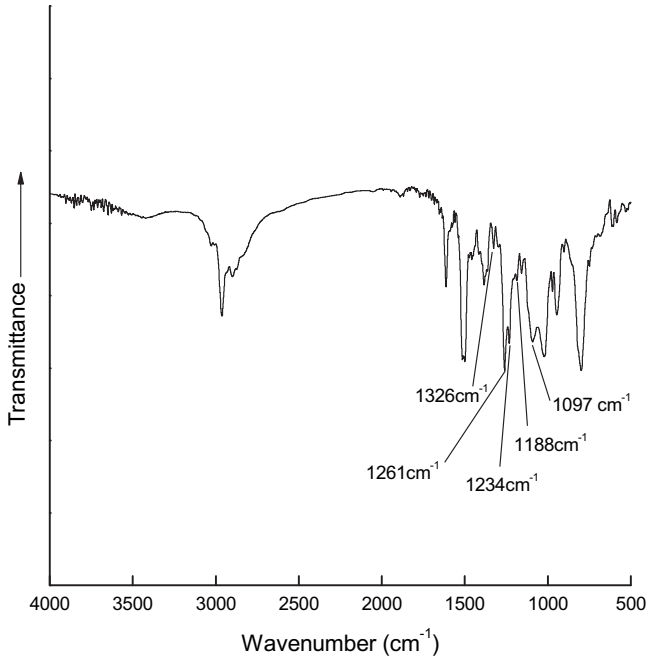


**Fig. 1.** FTIR spectra of PBaDDM54-*block*-PDMS multiblock copolymer.

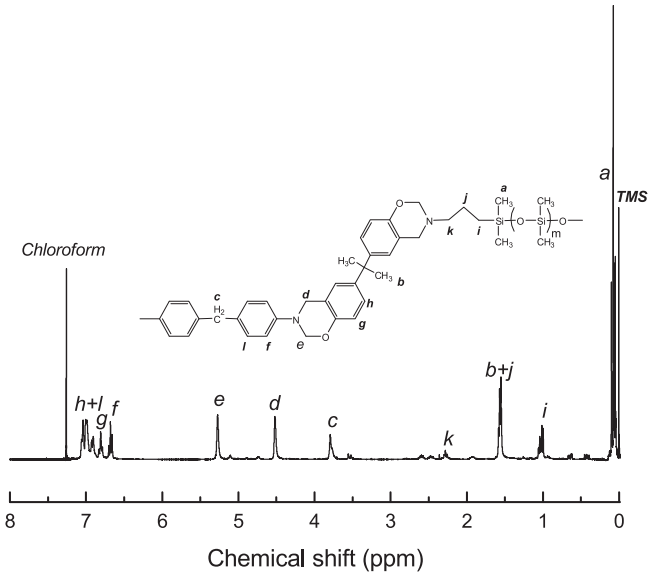


**Fig. 2.** $^1$H NMR spectra of PBaDDM54-*block*-PDMS multiblock copolymer.

reactivity of terminal functional groups in the macromers. The similar results have been obtained for the polymerization of other macromers [33].

### 3.2. Nanostructures of PBaDDM-b-PDMS multiblock copolymers

All the PBaDDM-*b*-PDMS multiblock copolymers obtained are homogeneous and transparent. The transparency implies that no macroscopic phase separation occurred within the multiblock copolymers. This observation is in marked contrast to the case of PBaDDM and PDMS blends, in which the macroscopic phase separation existed owing to the immiscibility of PBaDDM with PDMS. It is proposed that the multiblock copolymers are microphase-separated since the immiscible PBaDDM and PDMS blocks were combined with the covalent bonds. It is of interest to note that when the content of PDMS is lower than 50 wt% the PBaDDM-*b*-PDMS multiblock copolymers behaved as the tough plastics whereas the copolymers containing PDMS more than 50 wt% were the elastomers. The physical appearance of the multiblock copolymers could be associated with the formation of microphase-separated morphologies, in which the PBaDDM blocks were formed into either dispersed or continuous microdomains depending on the content of PDMS block.

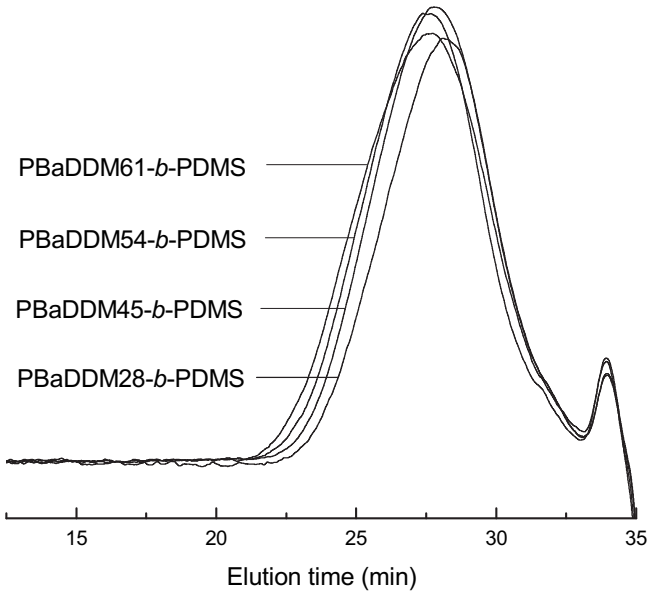


**Fig. 3.** GPC curves of PBaDDM-*block*-PDMS multiblock copolymers.

The microphase-separated morphology was investigated by means of atomic force microscopy (AFM) and small-angle X-ray scattering (SAXS). All the multiblock copolymers were cured at the elevated temperature and the cured samples were trimmed with an ultrathin microtome machine. The specimens of the section were subjected to the morphological observation. Shown in Fig. 4 are the AFM images of the samples. The left and right sides are the topography and phase images, respectively. It is seen that all multiblock copolymers exhibited the nanostructured morphologies. In the term of the difference in viscoelastic properties and volume fraction of the two kinds of blocks (*viz.* PDMS and PBaDDM) the dark region is attributed to the PDMS domains whereas the light region to the polybenzoxazine networks. For PBaDDM28-*b*-PDMS and PBaDDM45-*b*-PDMS, the worm-like nanodomains of PDMS were dispersed in the continuous polybenzoxazine matrices as shown in Fig. 4A and B. With increasing the content of PBaDDM, the interconnected PDMS nanodomains gradually transformed into some individual spherical partials and the size of PDMS nanodomains decreased (See Fig. 4C and D).

The morphologies of the PBaDDM-*b*-PDMS multiblock copolymers were further investigated by SAXS and the SAXS profiles are shown in Fig. 5. For all the multiblock copolymers, the well defined scattering peak was displayed in the extent of $q = 0.10$–$0.30$ nm$^{-1}$, indicating that the PBaDDM-*b*-PDMS multiblock copolymers were indeed microphase-separated. The microphase-separated morphology results from the immiscibility of the component blocks due to the big difference in solubility parameters between the PBaDDM and PDMS. According to the position of the primary scattering peaks the average distance between neighboring PDMS nanodomains can be estimated according to Bragg equation ($L = 2\pi/q_m$) as indicated in each SAXS profile. It is seen that the long period increased with increasing the content of PBaDDM.

### 3.3. Curing behavior

All the PBaDDM-*b*-PDMS multiblock copolymers were capable to dissolving in common solvents such as THF, chloroform and benzene, suggesting that no crosslinked structures were formed during the Mannich polycondensation. When heated up to elevated temperatures (*e.g.,* 200 °C) for some time, these PBaDDM-*b*-PDMS multiblock copolymers were no longer soluble in these solvents, suggesting that the multiblock copolymers were crosslinked. The crosslinking structures results from the thermally-activated ring-opening polymerization of benzoxazine ring in the main chains as depicted in the Scheme 2. The curing behavior of the multiblock copolymers was investigated in terms of non-isothermal curing kinetics by means of differential scanning calorimetry (DSC). The samples were heated from 140 to 300 °C at the different heating rates of 2, 5, 10, 15 and 20 °C/min. Representatively shown in Fig. 6 are the DSC thermographs of PBaDDM54-*b*-PDMS. At each heating rate, the curing of the polymeric precursors displayed a single exothermic peak. The exothermic peak resulted from the ring-opening polymerization of main-chain type polybenzoxazine blocks. Herewith, we define the onset ($T_i$) and peak ($T_p$) temperatures to account for the starting and maximum temperatures of each exothermic peak, respectively. The values of heat of reaction ($\Delta H$), $T_i$ and $T_p$ of the curing reaction are summarized in Table 2. As expected, the $T_i$'s and $T_p$'s increased with increasing the heating

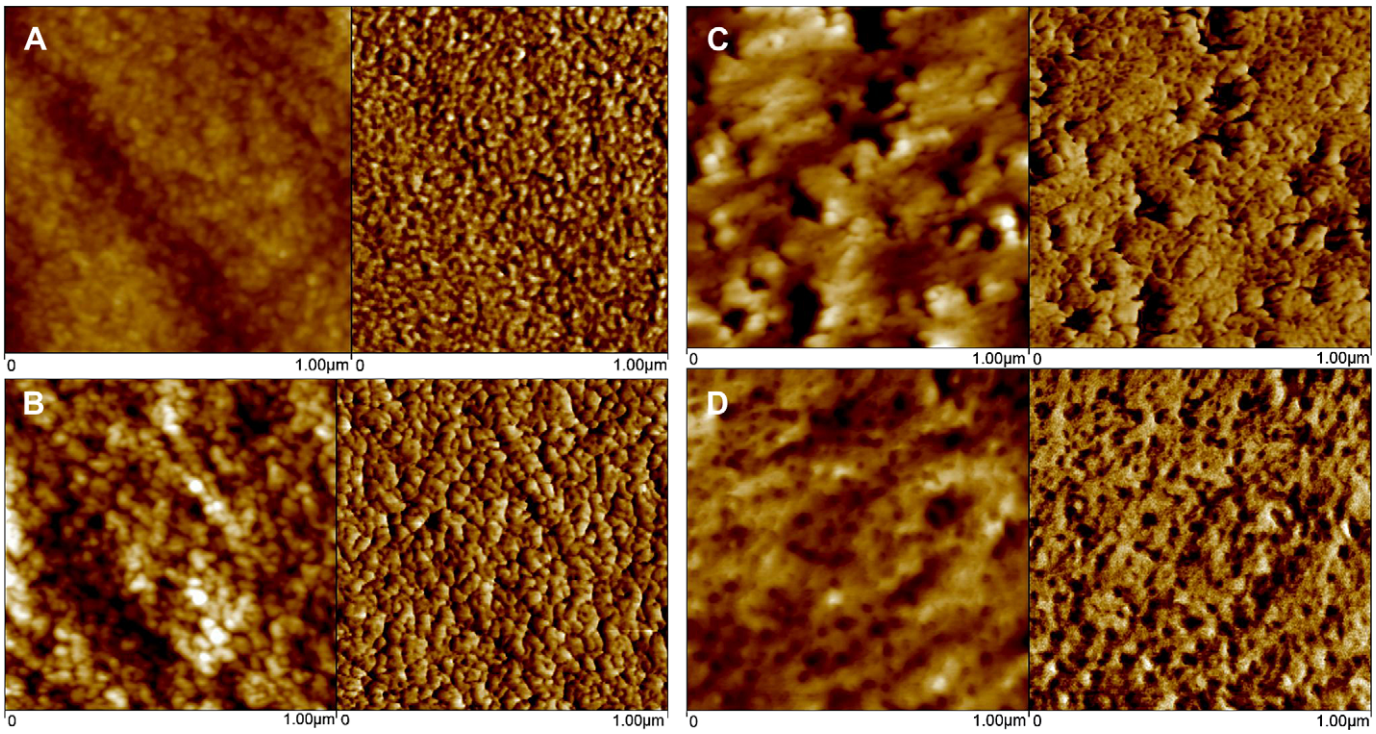


**Fig. 4.** AFM images of PBaDDM-*block*-PDMS multiblock copolymers. Left: height image, Right: phase image. A) PBaDDM28-*b*-PDMS, B) PBaDDM45-*b*-PDMS, C) PBaDDM54-*b*-PDMS, D) PBaDDM61-*b*-PDMS multiblock copolymers.

rates. The exothermic peaks of curing reaction increasingly became broad at the higher heating rates. It is noted that at the identical heating rate, the PBaDDM54-*b*-PDMS multiblock copolymer possessed higher $T_i$ and $T_p$ than the plain PBaDDM. This observation could be associated with the formation of the microphase-separated morphology in the multiblock copolymer. It is proposed that the presence of PDMS microdomains in the materials could interrupt the structural continuation of polybenzoxazine matrix and thus the enhanced temperatures were required to facilitate the

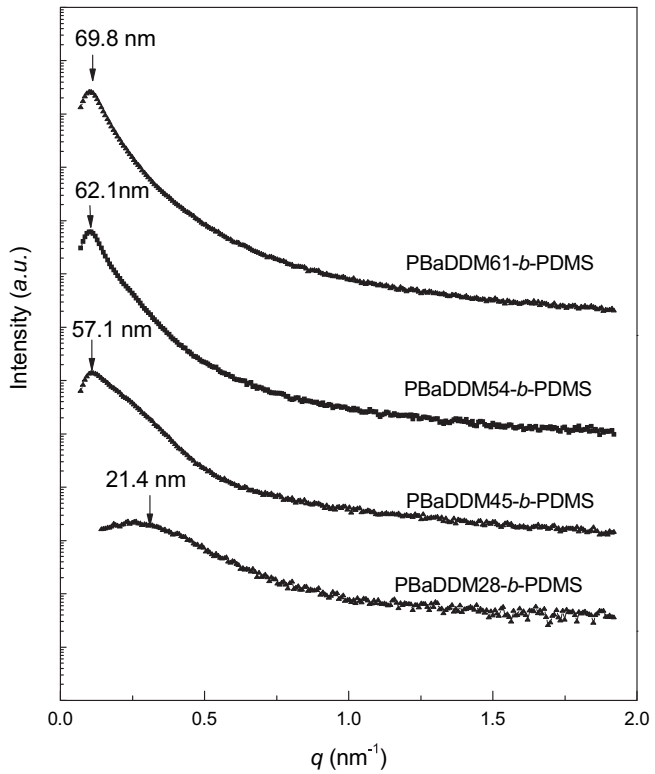


**Fig. 5.** SAXS profiles of PBaDDM-*b*-PDMS multiblock copolymers.

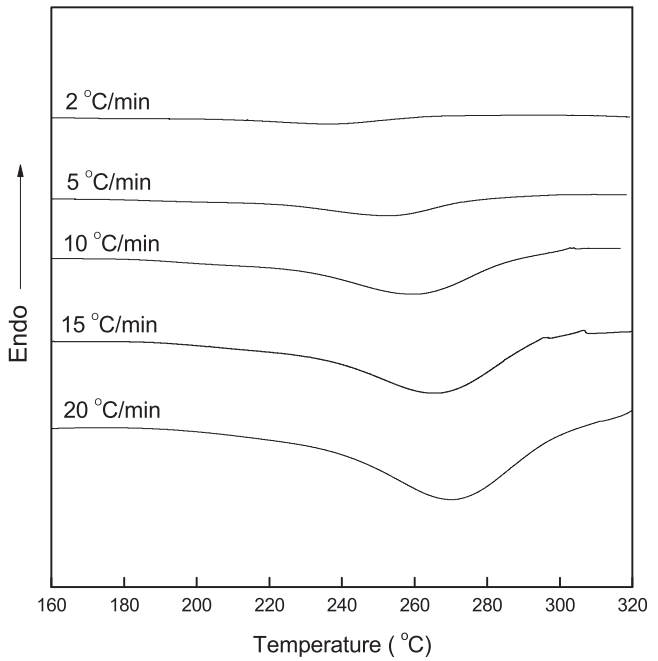


**Fig. 6.** Non-isothermal DSC thermographs of PBaDDM54-*b*-PDMS multiblock copolymer at different heating rates.

**Table 2**
Data of non-isothermal DSC curing kinetics for PBaDDM and PBaDDM54-*b*-PDMS.

| | $\beta$ (°C/min) | $T_i$ (°C)[a] | $T_p$(°C)[b] | $\Delta H$ (J/g)[c] |
|---|---|---|---|---|
| PBaDDM | 2 | 170.9 | 221.1 | 192.1 |
| | 5 | 159.7 | 235.4 | 210.8 |
| | 10 | 175.4 | 242.9 | 209.0 |
| | 15 | 184.6 | 249.3 | 200.0 |
| | 20 | 180.2 | 254.1 | 214.8 |
| PBaDDM54-*b*-PDMS | 2 | 164.1 | 236.8 | 205.6 |
| | 5 | 177.8 | 252.2 | 233.3 |
| | 10 | 180.5 | 259.9 | 230.0 |
| | 15 | 182.5 | 266.4 | 226.5 |
| | 20 | 184.4 | 270.4 | 232.0 |

[a] Onset temperature of curing exothermic transition.
[b] Peak temperature of curing exothermic transition.
[c] Enthalpy of curing reaction.

diffusion of polybenzoxazine bocks to achieve the crosslinking reaction. For the plain PBaDDM, the heat of reaction is about 210 J/g, which is slightly higher than the value (*i.e.*, 189 J/g) measured by Takeichi et al. [24]. As expected, the presence of inert PDMS domains would give rise to the depression in the heat of reaction. It is seen that at the identical heating rate, the $\Delta H$ values of the multiblock copolymers are significantly lower than that of the plain PBaDDM. It should be pointed out that the heat of reaction measured at the lower heating rate (*e.g.*, 5 °C/min) was quite lower than those measured at the higher heating rates. Ideally, the heat of reaction should be constant for the given sample irrespective of heating rate. Nonetheless, at slow heating rates some of the heat generated at the beginning or at the end of the reaction was hardly recorded because of lack of sufficient sensitivity of calorimeter [34].

With the above data of non-isothermal DSC scans at different heating rate, it is possible to estimate the activation energy of the curing reactions for the plain PBaDDM and PBaDDM54-*b*-PDMS multiblock copolymer. Kissinger and Ozawa approaches can be employed toward this end [35,36]. The Kissinger equation [35] can be represented by the Eq. (1):

$$\ln\left(\frac{\beta}{T_p^2}\right) = \ln\left(\frac{Q_P AR}{E_a}\right) - \frac{E_a}{RT_p} \tag{1}$$

where $\beta$ is the heating rate and $T_p$ is the temperature of exothermic maximum. $E_a$ is activation energy, $R$ is the universal gas constant and $A$ is the pre-exponential factor. $Q_p$ is defined as:

$$Q_p = -[df(\alpha)/d\alpha]_{\alpha=\alpha_p} \tag{2}$$

where $\alpha$ is the extent of the reaction (conversion degree), $f(\alpha)$ is the differential conversion function depending on the reaction mechanism [37]. For the curing reaction of thermosets, this approach assumes that the extent of the reaction at the temperature of exothermic peak is constant, independent of heating rates. The activation energy ($E_a$) of reaction can be determined according to the linear plot of the logarithm of $\beta/T_p^2$ versus the inverse of the peak temperature of the exothermic curing reaction (See Figs. 7 and 8). The Ozawa method [36] is another approach of dynamic curing kinetics without assuming any model. Its general expression can be represented by Eq. (3):

$$\ln\beta = \ln\left(\frac{AE_a}{R}\right) - \ln F(\alpha) - 5.331 - 1.052\left(\frac{E_a}{RT}\right) \tag{3}$$

$F(\alpha)$ is a constant function and defined as:

$$F(\alpha) = \int_0^{\alpha} \frac{d\alpha}{f(\alpha)} \tag{4}$$

The plots of the logarithm of $\beta/T_p^2$ or $\beta$ versus the reversal of the exothermic peak temperature are shown in Figs. 7 and 8. The good linear relationships for both the Kissinger and the Ozawa methods were obtained for the plain PBaDDM and PBaDDM54-*b*-PDMS, indicating the validity of the two approaches and thus the activation energy values for the curing of the plain PBaDDM and PBaDDM54-*b*-PDMS can be calculated from the slopes of the plots. In terms of Kissinger and Ozawa approaches, the values of $E_a$ for the plain PBaDDM were obtained to be 136 and 141 KJ/mol, respectively. The values of the activation energy for the plain PBaDDM were significantly higher than values of Ba monomer reported in the literature [34,37,38]. For the PBaDDM54-*b*-PDMS multiblock copolymer, the vales of $E_a$ were obtained to be 146 and 152 KJ/mol, respectively. It is noted that the values of activation energy of

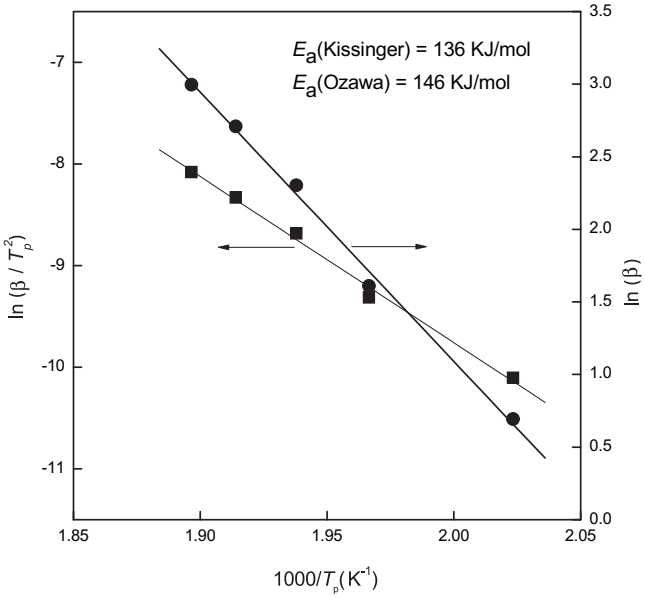


**Fig. 7.** Kissinger and Ozawa plots for the determination of activation energy of curing reaction for the plain PBaDDM.

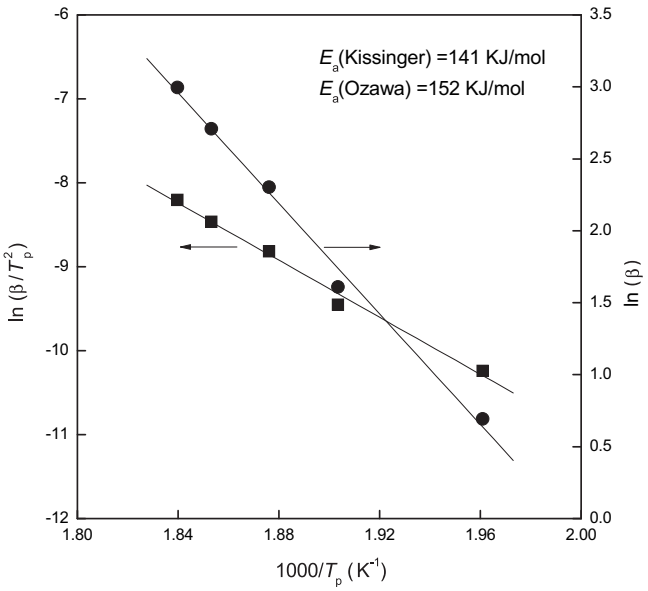


**Fig. 8.** Kissinger and Ozawa plots for the determination of activation energy of curing reaction for PBaDDM54-*b*-PDMS multiblock copolymer.

reaction for PBaDDM54-*b*-PDMS multiblock copolymer are higher than that of the plain PBaDDM, suggesting that the inclusion of the flexible block (*viz.* PDMS) gave rise to increased $E_a$, *i.e.,* the curing of the multiblock copolymers is to some extent more difficult than the plain PBaDDM. This result could be ascribed to the formation of the microphase-separated morphology in PBaDDM-*b*-PDMS multiblock copolymers. It is plausible to propose that the inert PDMS microdomains exerted a dilution effect on the ring-opening polymerization of polybenzoxazine matrices.

### 3.4. Thermal properties

Thermogravimetric analysis (TGA) was applied to evaluate the thermal stability of the cured PBaDDM-*b*-PDMS multiblock copolymers. The TGA curves of PBaDDM and the multiblock copolymers are shown in Fig. 9. The temperature at the weight loss of 5% was defined as the initial temperature of degradation ($T_d$). It is seen that with the inclusion of PDMS blocks, the initial temperature of degradation ($T_d$) was significantly decreased; the $T_d$ decreased with increasing the content of PDMS blocks. The decreased $T_d$ could result from the inclusion of the thermally labile aliphatic groups at the end of the PDMS blocks. For the thermoset from the plain PBaDDM, the char yield at 800 °C was 40.6%, which was significantly higher than the residue of degradation of PDMS at 800 °C (<5%) [39–41]. It is seen that the residue of degradation of the PDMS-containing thermosets decreased with increasing the content of PDMS. However, it is noted that when the content of PDMS is 46% or less, the residues of degradation of the thermosets are significantly higher than that of control thermosets from PBaDDM. This observation could be interpreted on the basis of the formation of microphase-separated morphology and the insulation effect of PDMS microdomains. For the thermosets with the content of PDMS less than 50 wt% the spherical PDMS microdomains were dispersed into the matrix of PBa thermosets; while the content of PDMS exceeds 50 wt%, the PBa microdomains were dispersed in PDMS matrix (See Fig. 4C). The increased residues of degradation for the thermosets from the multiblock copolymer containing PDMS less than 50% could be attributed to the formation of degradation products when the PDMS domains existed in the formation of nanosized domains and the insulation effect of PBa matrix on PDMS nanodomains. For the thermosets containing PDMS exceeding 50 wt%, the dispersed PBa microdomains would not protect the PDMS matrix from the thermal degradation. The similar results have been found in other siloxane-containing PBa hybrids [28,29,31].

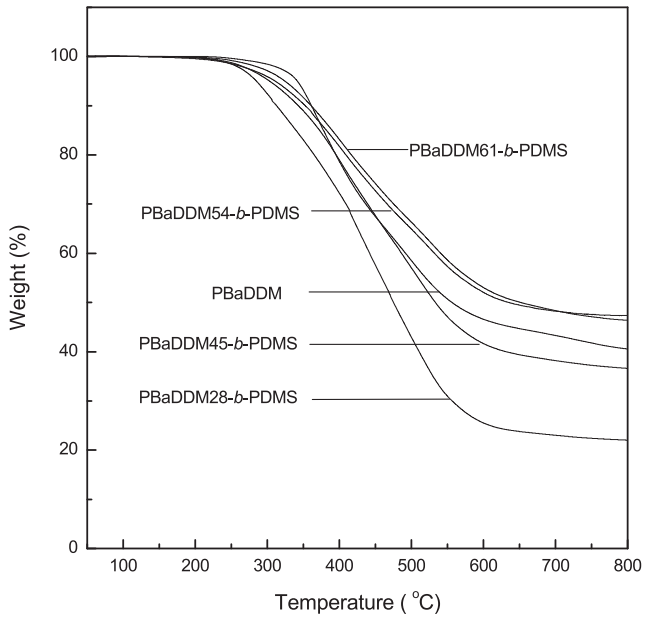


**Fig. 9.** TGA curves of PBaDDM-*b*-PDMS multiblock copolymers.

### 3.5. Surface properties

As an organosilicon polymer, PDMS is generally of low surface energy [42]. Therefore, the modification of polybenzoxazine materials with PDMS would be accompanied with the improvement in surface hydrophobilicity. In the present case, the PBaDDM and PDMS blocks are combined with covalent bonds and it is expected that the surface hydrophobicity (or dewettability) would be enhanced compared to the unmodified PBa thermosets. The specimens of films for the samples were prepared *via* spin-coating technique. The free surfaces of the multiblock copolymers were obtained and analyzed in terms of the measurement of static contact angle. Contact angles were measured with water and ethylene glycol as probe liquids and the results are summarized in Table 3. The contact angle of the cured PBaDDM was estimated with water to be *ca.* 95.4°. With the inclusion of PDMS block, the contact angle significantly increased. The contact angles of the multiblock copolymers increased with increasing the content of the PDMS blocks. For PBaDDM28-*b*-PDMS multiblock copolymers, the contact angle was measured to be 102.7° with water as the probe liquid. This increased contact angle indicates the hydrophobicity of materials was significantly increased; *i.e.,* the surface energy of materials was reduced. The surface free energies of the PBaDDM-*b*-PDMS multiblock copolymers can be calculated according to the geometric mean model [43–45]:

$$\cos\theta = \frac{2}{\gamma_L}\left[\left(\gamma_L^d\gamma_S^d\right)^{\frac{1}{2}}+\left(\gamma_L^p\gamma_S^p\right)^{\frac{1}{2}}\right]-1 \quad (5)$$

$$\gamma_S = \gamma_S^d + \gamma_S^p \quad (6)$$

where $\theta$ is contact angle and $\gamma_L$ is the liquid surface tension; $\gamma_L^p$ and $\gamma_L^d$ are the polar and dispersive components of $\gamma_L$, respectively. The calculated results of surface energy are also incorporated into Table 3. The non-polar component (*i.e.*, $\gamma_S^d$) seems to be more sensitive than the polar component (*i.e.*, $\gamma_S^p$) to the concentration of the PDMS, suggesting that the inclusion of PDMS significantly increased the distribution of the non-polar groups on the surface energy of materials; *i.e.,* the distribution of PDMS blocks on the surface was increased. The PDMS on the surface acted as a screening agent to reduce the surface energy of the multiblock copolymers. It is noticed that the values of the total surface free energy for the PBaDDM-*b*-PDMS multiblock copolymers were significantly lower than that of the plain PBaDDM. It should be pointed out that the surface

**Table 3**
Static contact angles and surface free energy of the cured PBaDDM-*b*-PDMS multiblock copolymers.

| Samples | Static contact angle (°) | | Surface free energy (mN × m$^{-1}$) | | |
|---|---|---|---|---|---|
| | $\theta_{H2O}$ | $\theta_{ethylene\ glycol}$ | $\gamma_S^d$ | $\gamma_S^p$ | $\gamma_S$ |
| PBaDDM | 95.4 ± 1.0 | 71.3 ± 1.2 | 21.09 | 2.61 | 23.70 |
| PBaDDM28-*b*-PDMS | 102.7 ± 1.2 | 82.5 ± 1.4 | 15.14 | 2.05 | 17.19 |
| PBaDDM45-*b*-PDMS | 99.5 ± 0.7 | 83.7 ± 1.0 | 10.37 | 4.62 | 14.99 |
| PBaDDM54-*b*-PDMS | 99.6 ± 0.5 | 86.1 ± 1.2 | 8.08 | 5.71 | 13.78 |
| PBaDDM61-*b*-PDMS | 99.4 ± 0.1 | 83.1 ± 0.5 | 10.91 | 4.43 | 15.34 |

Water: $\gamma_L$ = 72.8 mN/m, $\gamma_L^d$ = 21.8 mN/m, $\gamma_L^p$ = 51.0 mN/m [Ref. [43–45]] Ethylene glycol: $\gamma_L$ = 48.3 mN/m, $\gamma_L^d$ = 29.3 mN/m, $\gamma_L^p$ = 19.0 mN/m [Ref. [43–45]] PDMS: $\theta_{H2O}$ = 105–100° [Ref. [57,58]].

hydrophobilicity of the multiblock copolymers before curing reaction were also examined. It was found that the curing reaction did not significantly change the values of water contact angles, suggesting that the surface morphology and composition of the block copolymers remain almost invariant. It must be stressed that the surface hydrophobicity of the PDMS-containing PBa thermosets could additionally reflect change in surface roughness (and/or surface topology) resulting from the formation of the microphase-separated structures [46–54] or the change in intermolecular or intramolecular specific interactions in the organic-inorganic hybrid PBa thermosets [55,56].

## 4. Conclusions

The polybenzoxazine-*block*-polydimethylsiloxane multiblock copolymers containing main-chain polybenzoxazine were synthesized *via* the Mannich polycondensation among BPA, DDM, aminopropyl-terminated polydimethylsiloxane and paraformaldehyde. The multiblock copolymers were characterized by means of Fourier transform infrared spectroscopy (FTIR), nuclear magnetic resonance spectroscopy (NMR) and gel permeation chromatography (GPC). The multiblock copolymers displayed microphase-separated morphology as investigated by means of atomic force microscopy (AFM) and small-angle X-ray scattering (SAXS). Owing to the presence of the main-chain polybenzoxazine blocks, the multiblock copolymers are thermally-crosslinkable and their curing behavior was investigated in terms of the analysis of non-isothermal curing kinetics. The measurement of static contact angles showed that with the inclusion of polydimethylsiloxane blocks, the cured thermosets resulting from the multiblock copolymers displayed the improved surface hydrophobilicity compared to the plain polybenzoxazine thermosets.

## Acknowledgment

Financial support from Natural Science Foundation of China (No. 20474038 and 50873059) and National Basic Research Program of China (No. 2009CB930400) is gratefully acknowledged. The authors also thank Shanghai Leading Academic Discipline Project(Project Number: B202) for partial support.

## References

[1] Ghosh NN, Kiskan B, Yagci Y. Prog Polym Sci 2007;32:1344.
[2] Ning X, Ishida H. J Polym Sci Part A Polym Chem 1994;32:921.
[3] Ning X, Ishida H. J Polym Sci Part A Polym Chem 1994;32:1121.
[4] Laobuthee A, Chirachanchai S, Ishida H, Tashiro K. J Am Chem Soc 2001;123:9947.
[5] Holly FW, Cope AC. J Am Chem Soc 1944;66:1875.
[6] Kim HJ, Zdenka B, Ishida H. Polymer 1999;40:1815.
[7] Kim HD, Brunovska Z, Ishida H. Polymer 1999;40:6565.
[8] Ishida H, Lee YH. Polymer 2001;42:6971.
[9] Ishida H, Lee YH. J Polym Sci Part B Polym Phys 2001;39:736.
[10] Liu Y, Zhang W, Chen Y, Zheng S. J Appl Polym Sci 2006;99:927.
[11] Agag T, Takeichi T. Macromolecules 2001;34:7257.
[12] Tekeichi T, Zeidam R, Agag T. Polymer 2002;43:45.
[13] Agag T, Tsuchiya H, Takeichi T. Polymer 2004;45:7903.
[14] Brunovska Z, Liu J. Macromol Chem Phys 1999;200:1745.
[15] Su YC, Chen WC, Ou KL, Chang FC. Polymer 2005;46:3758.
[16] Liu Y, Zheng S. J Polym Sci Part A Polym Chem 2006;44:1168.
[17] Lee YJ, Kuo SW, Su YC, Chen JK, Tu CW, Chang FC. Polymer 2004;45:6321.
[18] Lee YJ, Kuo SW, Huang CF, Chang FC. Polymer 2006;47:4378.
[19] Riess G, Schwob JM, Guth G, Roche M, Lande B. Adv Polym Sci 1986;31:27.
[20] Velez-Herrera P, Doyama K, Abe H, Ishida H. Macromolecules 2008;41:9704.
[21] Chernykh A, Agag T, Ishida H. Polymer 2009;50:3153.
[22] Nakamura M, Ishida H. Polymer 2009;50:2688.
[23] Agag T, Jin L, Ishida H. Polymer 2009;50:5940.
[24] Takeichi T, Kano T, Agag T. Polymer 2005;46:12172.
[25] Agag T, Takeichi T. J Polym Sci Part A Polym Chem 2007;45:1878.
[26] Chernykh A, Liu J, Ishida H. Polymer 2006;47:7664.
[27] Agag T, Takeichi T. In: 12th International IUPAC conference on polymers and organic chemistry (POC'06). Okazaki, Japan; July 2, 2006.
[28] Arhyananta H, Haniff Wahid M, Sasaki M, Agag T, Kawauchi T, Ismail H, et al. Polymer 2008;49:4585.
[29] Ardhyananta H, Kawauchi T, Ismail H, Takeichi T. Polymer 2009;50:5959.
[30] Takeichi T, Agag T, Zeidam T. J Polym Sci Part A Polym Chem 2001;39:2633.
[31] Kiskan B, Aydigan B, Yagci Y. J Polym Sci Part A Polym Chem 2009;47:804.
[32] Wang L, Gong W, Zheng S. Polym Int 2009;58:124.
[33] Hargadon MT, Davey EA, McIntyre TB, Gnanamgari D, Wynne CM, Swift RC, et al. Macromolecules 2008;41:741.
[34] Ishida H, Rodrigues Y. Polymer 1996;36:3151.
[35] Kissinger HE. Anal Chem 1957;29:1702.
[36] Ozawa TJ. Therm Anal 1970;2:301.
[37] Jubsilp C, Damrongsakkul S, Takeichi T, Rimdusit S. Thermochim Acta 2006; 447:131.
[38] Yei DR, Fu HK, Chen WY, Chang FC. J Polym Sci Part B Polym Phys 2006;44:347.
[39] Tiwari A, Nema AK, Das CK, Nema SK. Thermochim Acta 2004;417:133.
[40] Ciolino AE, Villar MA, Valles EM, Hadjichristidis N. J Polym Sci Part A Polym Chem 2007;45:2726.
[41] Liu Y-L, Li S-H. Macromol Rapid Commun 2004;25:1392.
[42] Yilgor I, McGrath JE. Adv Polym Sci 1988;86:1.
[43] Kaelble DH, Uy KC. J Adhes 1970;2:50.
[44] Kaelble DH. Physical chemistry of adhesion. New York: Wiley-Interscience; 1971.
[45] Adamson AW. Physical chemistry of surfaces. 5th ed. New York: Wiley-Interscience; 1990.
[46] Shibuichi S, Onda T, Satoh N, Tsujii K. Langmuir 1996;12:2125.
[47] Barthlott W, Neinhuis C. Planta 1997;202:1.
[48] Li H, Wang X, Song Y, Liu Y, Li Q, Jiang L, et al. Angew Chem Int Ed 2001;40: 1743.
[49] Feng L, Li S, Li Y, Li H, Zhang L, Zhai J, et al. Adv Mater 2002;14:1857.
[50] Gao XF, Jiang L. Nature 2004;432:36.
[51] Shirtcliffe NJ, McHale G, Newton MI, Perry CC. Langmuir 2003;19:5626.
[52] Zhang X, Shi F, Yu X, Liu H, Fu Y, Wang ZQ, et al. J Am Chem Soc 2004;126:3064.
[53] Han JT, Xu XR, Cho KW. Langmuir 2005;21:6662.
[54] Feng J, Jiang L. Adv Mater 2006;18:3063.
[55] Wang CF, Su YC, Kuo SW, Huang CF, Sheen YC, Chang FC. Angew Chem Int Ed 2006;118:2306.
[56] Liao CS, Wang CF, Lin HC, Chou HY, Chang FC. Langmuir 2009;25:3359.
[57] Seo J-H, Matsuno R, Konno T, Takai M, Ishihara K. Biomaterials 2008;29:1367.
[58] Zhang X, Lin G, Kumar SR, Mark JE. Polymer 2009;50:5414.